Tides in the northern Adriatic Sea — the Gulf of Trieste

V. Malačič[1] and D. Viezzoli[2]

[1] *National Institute of Biology, Marine Biological Station Piran, Fornače 41*
    6330 Piran, Slovenia
[2] *Istituto Nazionale di Oceanografia e Geofisica Sperimentale (OGS)*
    Borgo Grotta Gigante 42/C, 34010 Sgonico, Trieste, Italy

Summary. — The effects of tides in the northern Adriatic Sea were examined using the 2D finite-difference model. The Eulerian residual velocity field of the calibrated model was checked for the mixing efficiency of tides in the northern Adriatic Sea. It is shown through the simulation of tides for the period of one half year that tides are too weak to mix the whole water column (at any time within this period), even in front of the promontories (*e.g.* the Po river outlet). The model resolution (556 m) allowed analysis of the tidal dynamics in smaller regions. In the Gulf of Trieste the model results are in satisfactory agreement with the current-meter observations for winter 1984-85 and spring 1985. It is shown that in the middle of the entrance to the gulf the sense of rotation of the tidal ellipse vector changes from a clockwise rotation at the southern part of the entrance to an anticlockwise rotation at the northern part of entrance. Tidal currents in the interior of the gulf rotate counterclockwise, while in small bays, and in front of them, the rotation is clockwise.

PACS 92.10.Hm – Surface waves, tides, and sea level.

1. – Introduction

Early studies on tidal dynamics of the Adriatic Sea began in the nineteenth century. Defant[1] showed that Mediterranean tides are strong in the northern part of the Adriatic Sea (the Gulf of Trieste). The tide there is of a mixed type, with the M_2 constituent prevailing and K_1 as the second most powerful one[2]. Taylor[3] described analytically the tidal dynamics of a rectangular semi-enclosed basin. His theory, however, does not apply to a domain around a co-oscillating gulf located at a side of the closed end of a basin (*e.g.*, the Gulf of Trieste). The problem of the absorption of semidiurnal tidal waves at the head of the basin (the coast from Venice to Trieste) was studied in[4]. The absorption displaces the amphidromic point towards the western (Italian) coast.

The early numerical models of the northern Adriatic Sea focused attention on the M_2 and the K_1 components[5] (2D model), and the M_2 alone[6] (3D model). In both models different boundary conditions were utilised.

The TRIM 2D model (Tidal, Residual, Intertidal Mudflat) model was adapted for the simulation of tides in the Northern Adriatic Sea and in the Gulf of Trieste. The model was first applied to the tidal dynamics of San Francisco Bay in California [7], and recently also to the northern Adriatic Sea [8]. The model results for the Gulf of Trieste were summarized in [9].

This paper will show how tides are efficient at mixing the water column in the northern Adriatic Sea, how well the model results match the current-meter observations in the Gulf of Trieste, and what the model results are along the open-boundary line of the gulf.

2. – Numerical model

The purpose of the model was to simulate accurately the tidal motion within the model sub-domain, which extends from about 20 km north of the open-boundary line towards the Gulf of Trieste. The open boundary line of the model, which is 124 km long, connects the past sea-level station Pesaro in Italy with the Kamenjak promontory in Croatia, the southernmost tip of the peninsula of Istria. Kamenjak is located near the past sea-level station Pula, as shown in fig. 1. The model topography was created
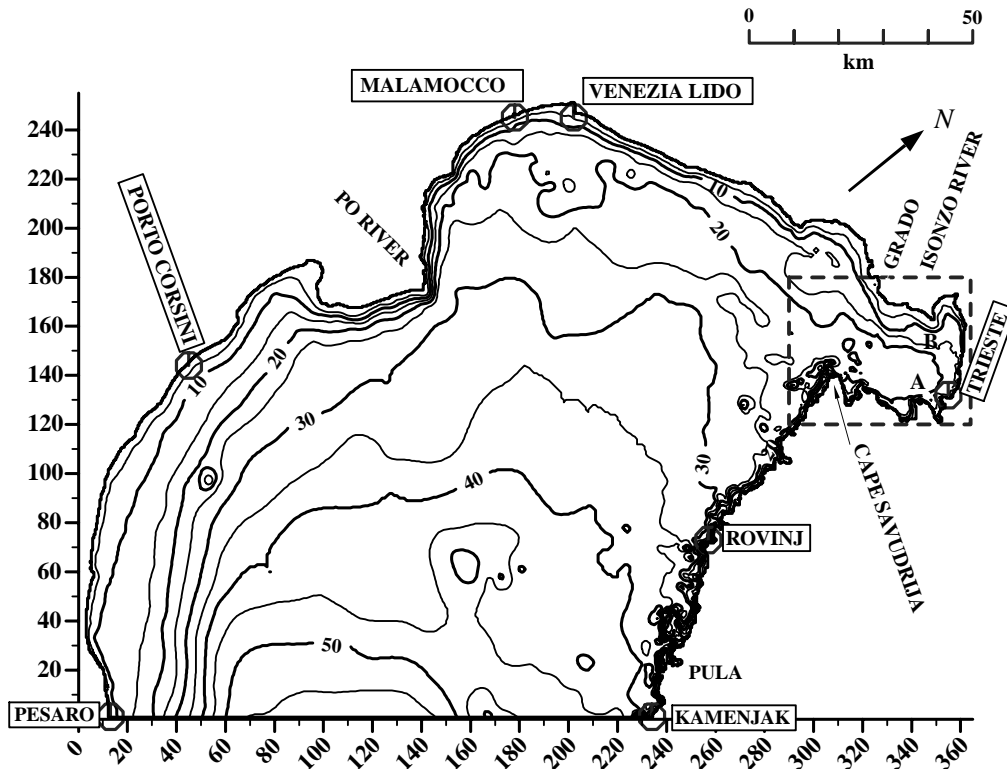

Fig. 1. – Model domain of the northern Adriatic Sea with its topography. The isobaths are in meters and the axes are in model units (1 unit = 555.6 m = 0.3 nautical miles). The inserted rectangle marks the model subdomain (the Gulf of Trieste).

from more than 6100 topographic data points and 3100 coastal data points, which were Kriging-interpolated. Each of the resulting square grid elements was 555.6 m wide.

The 2D finite-difference model is of a semi-implicit type and is unconditionally stable. A detailed description of the model can be found in [10] and [7]. The model solves the vertically-averaged equations of motion:

(1)
$$
\begin{cases}
\dfrac{du}{dt} - fv = -g\dfrac{\partial\eta}{\partial x} - \dfrac{g}{2\varrho_0}(D+\eta)\dfrac{\partial\overline{\varrho}}{\partial x} + v_H\Delta u + \dfrac{(\tau_x^0 - \tau_x)}{(D+\eta)\,\varrho_0}\,, \\[3mm]
\dfrac{dv}{dt} + fu = -g\dfrac{\partial\eta}{\partial y} - \dfrac{g}{2\varrho_0}(D+\eta)\dfrac{\partial\overline{\varrho}}{\partial y} + v_H\Delta v + \dfrac{(\tau_y^0 - \tau_y)}{(D+\eta)\,\varrho_0}\,,
\end{cases}
$$

together with the vertically integrated equation of continuity

(2)
$$
\frac{\partial\eta}{\partial t} = -\frac{\partial[(\eta+D)\,u]}{\partial x} - \frac{\partial[(\eta+D)\,v]}{\partial y}\,,
$$

where (u, v) is the vertically averaged (transport) velocity, η the sea-surface elevation (SSE) above the mean-level, D the depth, $f(= 1.04\cdot 10^{-4}\,\mathrm{s}^{-1})$ the Coriolis parameter, $\overline{\varrho}$ the vertically averaged density, ϱ_0 the reference density, v_H the coefficient of horizontal eddy viscosity, (τ_x^0, τ_y^0) the wind-stress at the surface, and (τ_x, τ_y) the bottom-friction stress. Density variations, horizontal diffusion of momentum, and wind-stress were all set to zero in tidal analysis. The system (1)-(2), which solves for the unknowns (u, v) and η, is nonlinear because of advection and bottom-friction terms. Bottom-friction stress is considered as a nonlinear function of transport velocity:

(3)
$$
\frac{\tau_x}{\varrho_0} = C_D u\sqrt{u^2 + v^2}\,, \qquad \frac{\tau_y}{\varrho_0} = C_D v\sqrt{u^2 + v^2}\,,
$$

where the drag coefficient C_D, known in oceanography, is related to the Chezy-Manning coefficient C_Z, used mainly in hydraulics [11]:

(4)
$$
C_D = \frac{g}{C_Z^2}\,.
$$

The coefficient C_D ranges from 0.002 to 0.003 for the bottom of the northern Adriatic Sea, which is composed of mud and mud/sand [11]. In shallow regions $(D < 4\,\mathrm{m})$, however, C_D is also a function of depth D. This dependence must be ascertained from the model results. For the determination of C_Z the open-boundary conditions, which consist of the prescribed SSE along the line Pesaro-Pula, need to be defined first. They were deduced from Polli's charts [2] using parabolic fits of amplitude and phase through the intersection points of cotidal and co-range lines with the open-boundary line [8]. From numerous runs of the model for the strongest semi-diurnal M_2 constituents the following relationship

(5)
$$
C_Z = C_0[2 - \exp[-D/D_0]]\,,
$$

where $C_0 = 40\,\mathrm{m}^{1/2}\,\mathrm{s}^{-1}$ and $D_0 = 2.5\,\mathrm{m}$, has proven to give the best SSE amplitude damping and phase retardation of the tidal M_2 wave in the port of Trieste. The friction coefficient has a value of $62\,\mathrm{m}^{1/2}\,\mathrm{s}^{-1}$ $(C_D = 2.55\cdot 10^{-3})$ when $D = 2\,\mathrm{m}$ and is almost depth

independent ($C_Z = 80 \text{ m}^{1/2} \text{ s}^{-1}$, $C_D = 1.53 \cdot 10^{-3}$) for $D > 12$ m, when the variations with depth are smaller than 0.4%. After determination of C_D, the open-boundary conditions were improved to obtain the best match with the sea-level observations in five ports (fig. 1): Rovinj, Trieste, Venezia-Lido, Malamocco and Porto Corsini [8].

    After the calibration of parameters and fine-tuning of the open-boundary conditions, the model was run for the first 190 days of the year 1985, when currents were measured in the Gulf of Trieste. The model was forced with the superposition of seven tidal constituents at the open-boundary line. The hourly values of SSE and of the transport velocity components were extracted from the model output. Every fifth model cell in both axis directions was considered in the analysis with the harmonic least-square fit using the "singular value decomposition" algorithm [12]. The Rayleigh criteria was fully respected—the synodic period for the separation of S_2 and K_2 is 182.6 days [13]. The nodal factors were imposed on amplitudes and phases according to [14] by adopting the algorithm from [15]. A spin-up period of 31 days was applied to avoid initial transients completely.

    The model calibration was rather successful, since we have achieved the root-mean square error of amplitudes of SSE of all seven most important tidal constituents in five ports to be smaller than 1 cm (0.5 cm $\pm$ 0.5 cm). Nearly the same results were obtained for the vectorial difference between the model and observed values: 0.8 cm $\pm$ 0.7 cm. The error of phase lag was less than 5° (4.4° $\pm$ 4.2°). Finer tuning would require a better determination of the observed values of harmonic constants.

3. – Tidal mixing in the northern Adriatic Sea

    Let us introduce a quantity P, which reflects the power of the stirring of tidal currents per unit of depth of the water column

$$(6) \qquad\qquad P = \log \left[\frac{(D + \eta)}{\varrho C_D |\mathbf{u}|^3} \right]_{\min},$$

where the density $\varrho = 1025 \text{ kg m}^{-3}$ was assumed. Lower P means a higher rate of kinetic energy for mixing the water column. The tidal stirring, proportional to $|\mathbf{u}|^3/(D + \eta)$, affects the rate of the potential energy anomaly ϕ

$$(7) \qquad\qquad \phi = \frac{1}{(D + \eta)} \int_{-D}^{\eta} (\bar{\varrho} - \varrho) \, gz \, dz,$$

which measures the depth averaged deficit of potential energy of a stratified water column with respect to the potential energy of a completely mixed water column with density $\bar{\varrho}$ [16]. Provided that the amount of kinetic energy which goes into turbulent kinetic energy is spatially uniform, P can be seen as a measure of tidal mixing capacity [16].

    The expression (6) is slightly different from the one used by Simpson and Hunter [17], but very close to that of Loder and Greenberg [18], in which the mean value of the argument in P was of interest. In this study, however, the tides in the northern Adriatic Sea were checked to see if they would be strong enough, at least once during the run-time period, to locally mix the water column. The required minimum of P for mixing the water column is either extracted from *in situ* oceanographic

observations or from remote-sensing images. However, it will be shown by model results that even without the determination of the minimum of P by these methods tides cannot mix the whole water column in the northern Adriatic Sea.

In the Irish Sea [17] and in the Gulf of Maine [18] P was successfully correlated with the position of thermal fronts, which lie on continental shelf areas between the well-mixed zones and the stratified zones. In the Gulf of Maine fronts were located where $P = P_c \cong 1.9$, while in the Irish Sea fronts were located where $\log(D/|\mathbf{u}|^3) \cong 2.7$ [19]. It follows from (6) that the latter condition gives $P_c \cong 2.5$ when $C_D = 1.53 \cdot 10^{-3}$ and $\eta = 0$. For continental shelf areas it was shown by [16] that the argument of P_c is inversely proportional to the vertical buoyancy flux, and for a thermally stratified water column to the absorbed heat flux. Since the Irish Sea and the English Channel have latitudes about 5° higher than the latitude of the model domain ($\cong 45°$), it is expected that $P_c < 2.5$ for the northern Adriatic area, since the amount of absorbed heat flux is larger than that absorbed in the Irish sea—the net annual incoming radiation in regions at a latitude around 45° is higher than the annual radiation in regions at a latitude around 50° for about 15 W/m² [20].

Hourly values of $|\mathbf{u}(t)|$ and η were retrieved from the model run simulating tides for 190 days. From the data of topography (D) the drag coefficient C_D was calculated from (3) and (4). At every grid point, P was obtained from (6) for the period of model simulation. In the plot of distribution of P (fig. 2) only every fifth point was considered
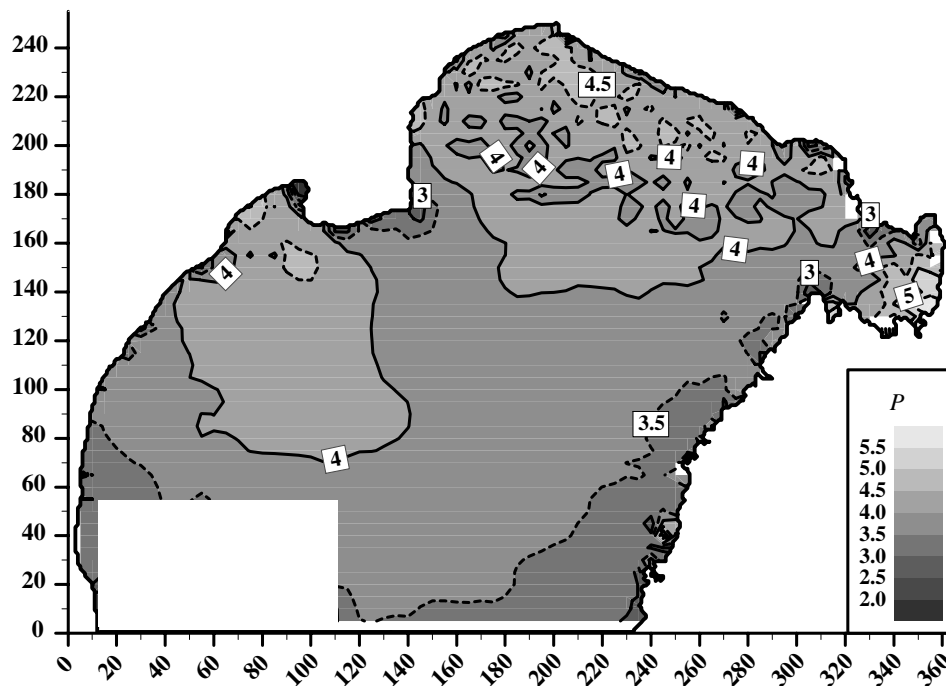

Fig. 2. – Distribution of mixing parameter P. The minimum of the argument of P has been taken at every grid point over the full period of simulation ($= 4560$ h), only every fifth point has been considered in the plot. Lower values of P, which mean higher tidal mixing capacity, are along the eastern coast, and in front of the Po river outflow. Values in the south-western corner of the domain are blanked, because they are generated artificially by the model open-boundary condition.

(the resolution is then 2778 m). Over the whole model domain $P > 2.5$, having lower values near the eastern coast (right-hand side boundary) and in front of the Po river mouth (fig. 2), where the tidal flow is locally accelerated. Although tidal currents are not strong enough to mix the whole water column, they are still far from being negligible: near the northern boundary, where $P \cong 4$, and $D \cong 20$ m ($\eta \ll D$), $|\mathbf{u}(t)| \cong$ 0.1 m/s. Around the south-western corner of the domain, model results in the region of extension smaller than 50 km are suspect, since they are generated as a side-effect of the model open-boundary condition [8].

4. – Model results and observations in the Gulf of Trieste

a) Model results

The model domain of the Gulf of Trieste is presented in fig. 3 and instantaneous SSE and transport velocity in spring tides at flood and ebb times are shown in fig. 4. The isolines of instantaneous SSE are aligned with the gulf's axis and with the vectors of transport velocity, indicating a prevalent standing-wave character of the tidal dynamics, except around Cape Savudrija, where a travelling component of a tidal wave is also present. The isolines of SSE diverge towards the northern and southern corners
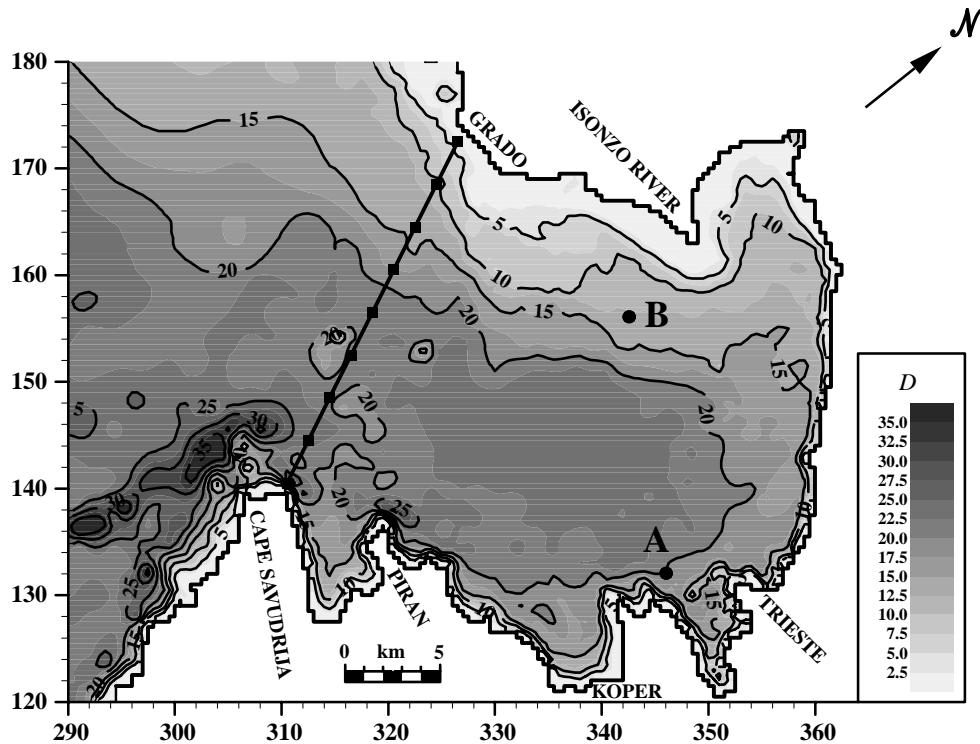

Fig. 3. – The model domain of the Gulf of Trieste with isobaths in meters. Model grid points at the entrance of the Gulf of Trieste, considered in analysis are represented by squares. The distance between the two neighbouring squares is 2.5 km. Locations of currentmeter observations (full circles) performed in 1984-1985 (site A) and in 1985 only (site B).
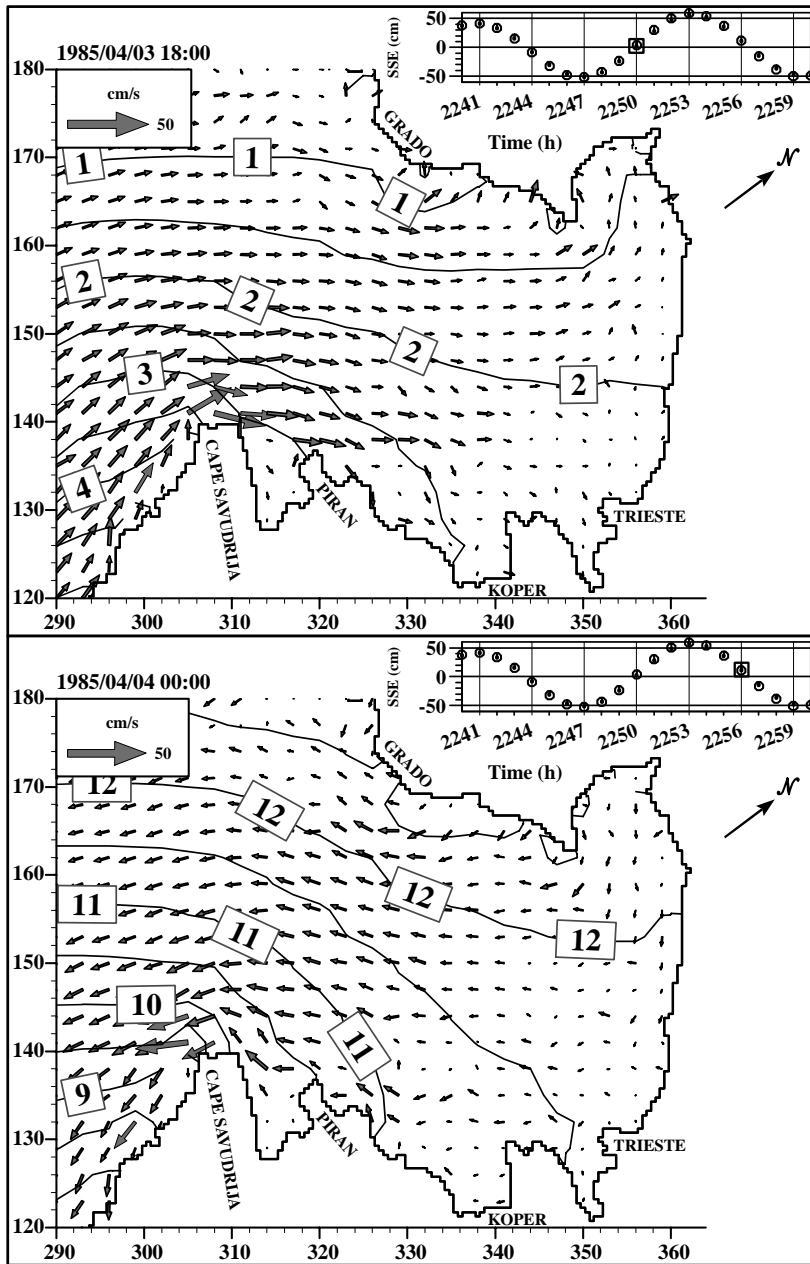
Fig. 4. – Tidal transport velocities (arrows) and SSE (isolines) at flood time (top) and at ebb time (bottom) in the Gulf of Trieste. All seven tidal constituents were combined. The isolines are in 10^{-2} m. The diurnal evolution of SSE in the port of Trieste is inserted at the top of the figures. Full circles: the sea-level prediction; empty circles: model results; rectangle: instantaneous SSE. Transport velocities were averaged over four neighbouring cells to smooth the sudden local changes in transport directions.

near the Gulf's closed end. The zone near Cape Savudrija is characterized by an enhanced inflow transport [9], where the maximum value of spring tides reaches 0.3 m/s in the vicinity of the tip. Model results have also shown that at the time of SSE maximum there is still a tidal inflow at the southern side and a tidal outflow at the northern side of the gulf's open boundary [9] and that at the times of SSE extremes in the port of Trieste the isolines of SSE are aligned with the closed end of the gulf. It also follows from fig. 4 that the SSE is always higher at the right-hand side of the transport, similar to the situation over the whole northern Adriatic Sea [8]. The model shows that the water mass transport into the gulf follows the rhythm of a standing wave, being slightly modulated across the gulf by the Coriolis force.

The transport velocity and SSE fields over the Gulf of Trieste would certainly be in error, especially near its southern side, if the gulf was modelled as a separate object and not as a part of the northern Adriatic Sea. The proper boundary conditions could not be guessed at correctly from just the numerical simulation, in which sea-level data from only one or two tide gauges would be available for tuning purposes (in the port of Trieste, and near it in the port of Koper).

The Gulf of Trieste is similar to a rectangular basin with a width $a = 20.4 \cdot 10^3$ m, length $b = 28.9 \cdot 10^3$ m, and with a trapezoidal cross-section of area $S = 3 \cdot 10^5$ m^2, where the northern half of the basin has a linear bottom profile, while the southern half is flat-bottomed with a depth of 20 m. From the conservation law of volume it follows

$$(8) \qquad\qquad \langle v \rangle = \frac{A}{S} \frac{\mathrm{d}\eta}{\mathrm{d}t} \,,$$

where $\langle v \rangle$ is the transport velocity averaged over the gulf's cross-section; $A = ab$ is the surface area of the gulf; and η is the SSE. The tidal range in the Gulf of Trieste is scaled as 1 m, therefore $\mathrm{d}\eta/\mathrm{d}t = 1\,\mathrm{m}/(6 \times 3600\ \mathrm{s})$. This gives a peak value of $\langle v \rangle \approx 0.09$ m/s. This simple estimate of transport velocity, without consideration of momentum, is surprisingly close to the results of the numerical model.

The ellipse eccentricity e was calculated according to [13], with the sign of the rotary coefficient [21]. For pure rectilinear motion $e = 1$, for circular motion $e = 0$. For clockwise motion $e > 0$, while for the counterclockwise motion $e < 0$. Model simulation showed that the distribution of the ellipse eccentricity e over the gulf is very similar for all major tidal constituents (M_2, S_2 and K_1). The distribution of e for the M_2 and K_1 constituents is shown in fig. 5, where the sign of e is taken from the rotary coefficient [21]. The tidal current rotates anticlockwise over the major part of the gulf—similar to the rotation of the tidal current over the northern Adriatic Sea [8]. This agrees with the findings in [22]. The anticlockwise rotation of tidal currents in the area near the closed end of the bays was explained in [23]. The sense of rotation of tidal current changes towards clockwise in front of embayments [13], as in front of the Bay of Piran (near cape Savudrija) and, in the Bays of Muggia (south of Trieste) and of Panzano (the northernmost bay of the gulf).

Finally, we explored the model results along the line cape Savudrija-Grado lagoon at the entrance of the Gulf of Trieste. Along the line Savudrija-Grado, nine equidistant grid cells were chosen for the horizontal profile of tides at the gulf's entrance (fig. 3). In fig. 6 the profiles of amplitudes of SSE, the eastern velocity component U, and the northern velocity component V, are shown. The amplitude of SSE increases slightly from Savudrija towards Grado (less than 0.3 cm for the major M_2 constituent). The amplitude of the eastern velocity component decreases in this direction, while the
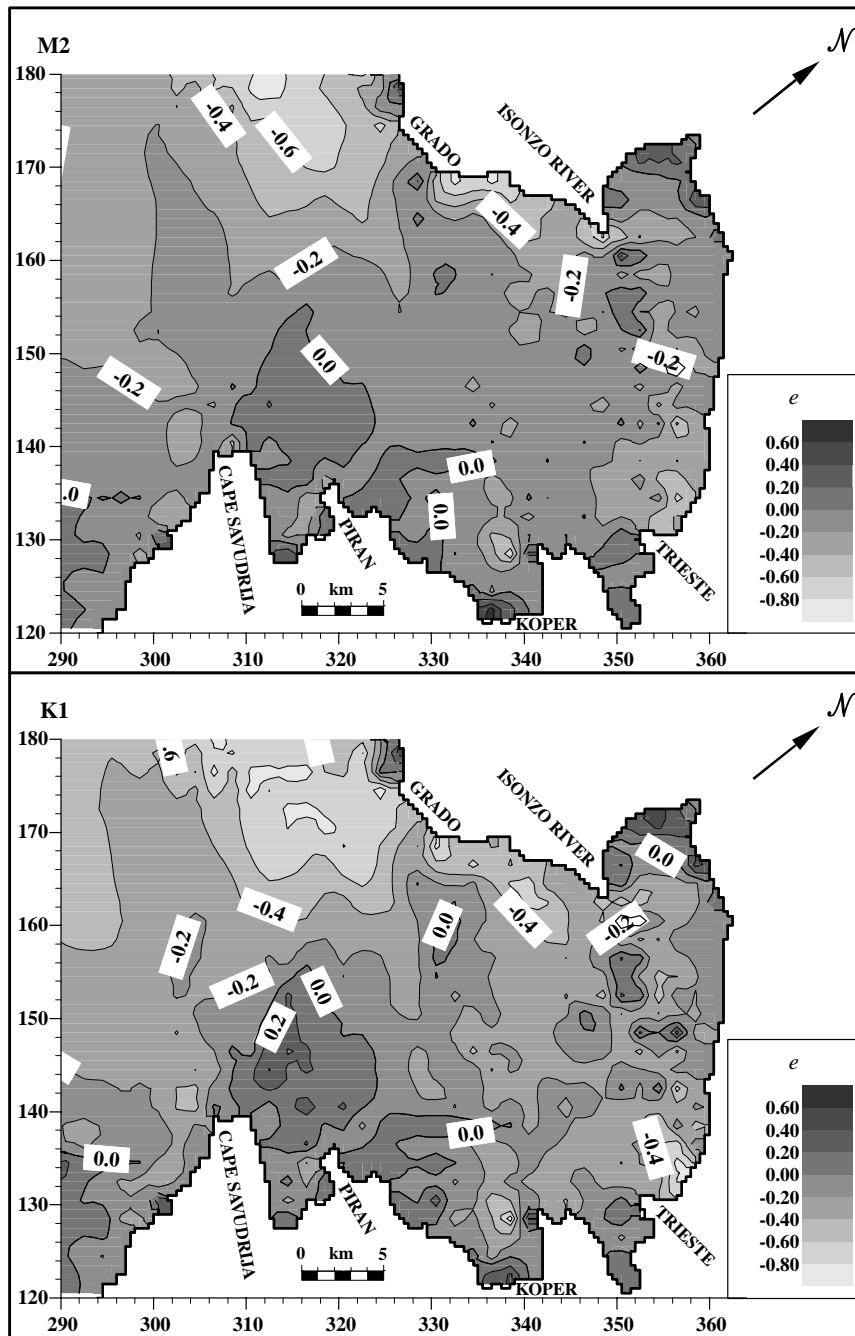
Fig. 5. – Ellipse eccentricity e of the M_2 tidal constituent (top), and of the K_1 constituent (bottom) in the Gulf of Trieste. The sign of e was taken from the rotary coefficient [21]. For pure rectilinear motion $e = 1$, for circular motion $e = 0$ [13], for clockwise motion $e > 0$ (shaded darkly), while for the counterclockwise motion $e > 0$ (shaded lightly).
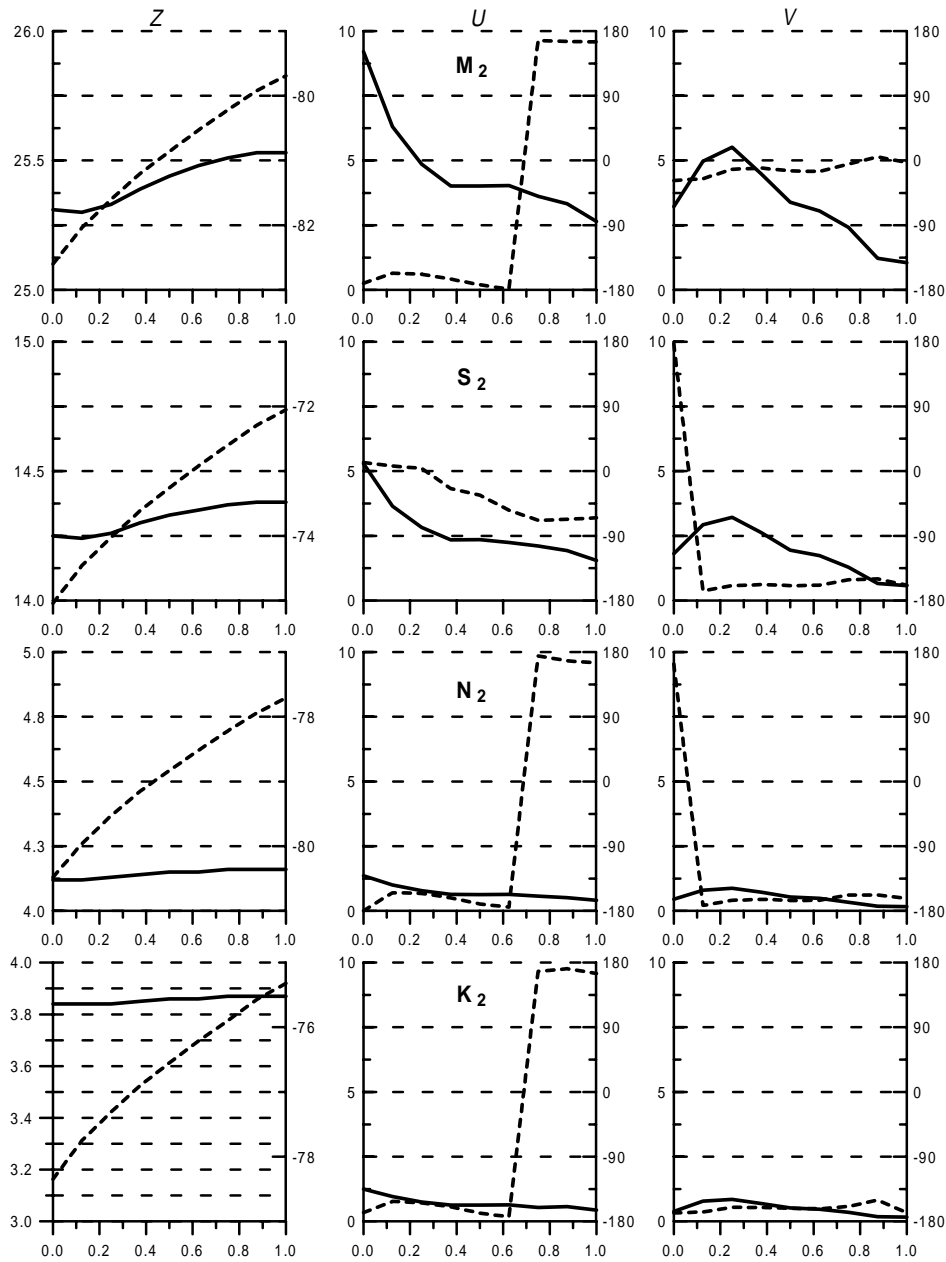
Fig. 6. – Profiles of amplitudes of SSE (Z), eastern (U) and northern velocity components (V) along the profile Savudrija-Grado for semidiurnal constituents. The horizontal axis represents the normalized distance from the first grid point near cape Savudrija towards the last one at the edge of Grado lagoon. The modulus of amplitude (full lines) is scaled at the left-hand side of each plot (in 10^{-2} m for Z, 10^{-2} m/s for U and V), while the argument (phase shift, dashed lines) is scaled at the right-hand side of each plot (in degrees).
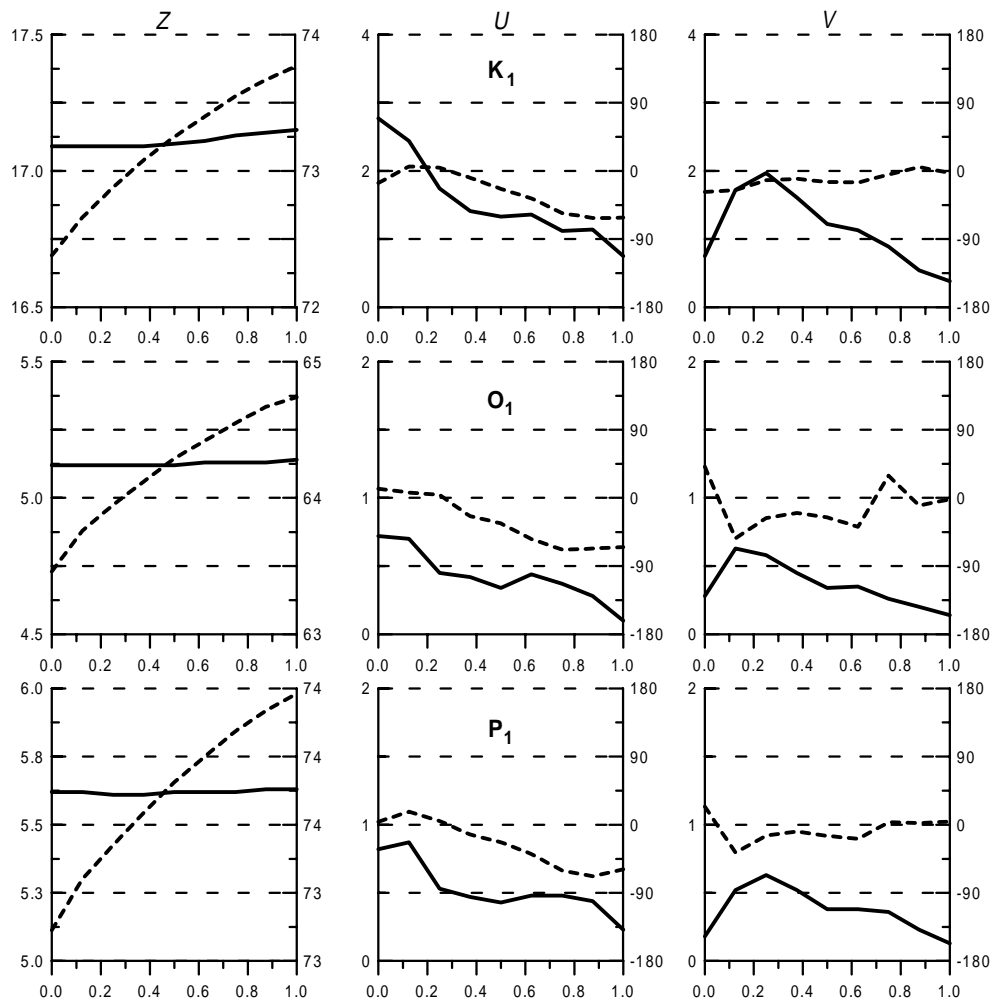
Fig. 6. – Continued for diurnal tidal constituents.

amplitude of the northern velocity component reaches a maximum about 8 km off Savudrija, near the central part of the gulf's entrance, where the orientation of tidal ellipses of all tidal constituents is close to 48° anticlockwise from east (fig. 7). The tidal current ellipses of all constituents are very narrow there and the sense of rotation of the tidal current changes from clockwise in the southern part of the gulf's entrance towards anticlockwise in the northern part. The phase shift of SSE changes slightly (fig. 6) for only a few degrees from the southern coast towards the northern coast of the gulf, but the phase shift of velocity components varies more pronouncedly, especially for the semidiurnal S_2 constituent and for diurnal constituents.

These results are appliable as the open-boundary conditions for future modelling, when the gulf is considered as a self-consistent domain. Tides in the Gulf of Trieste resemble in many ways tides of the northern Adriatic Sea, and could therefore be considered as its miniature [8]. There are, however, differences in the space
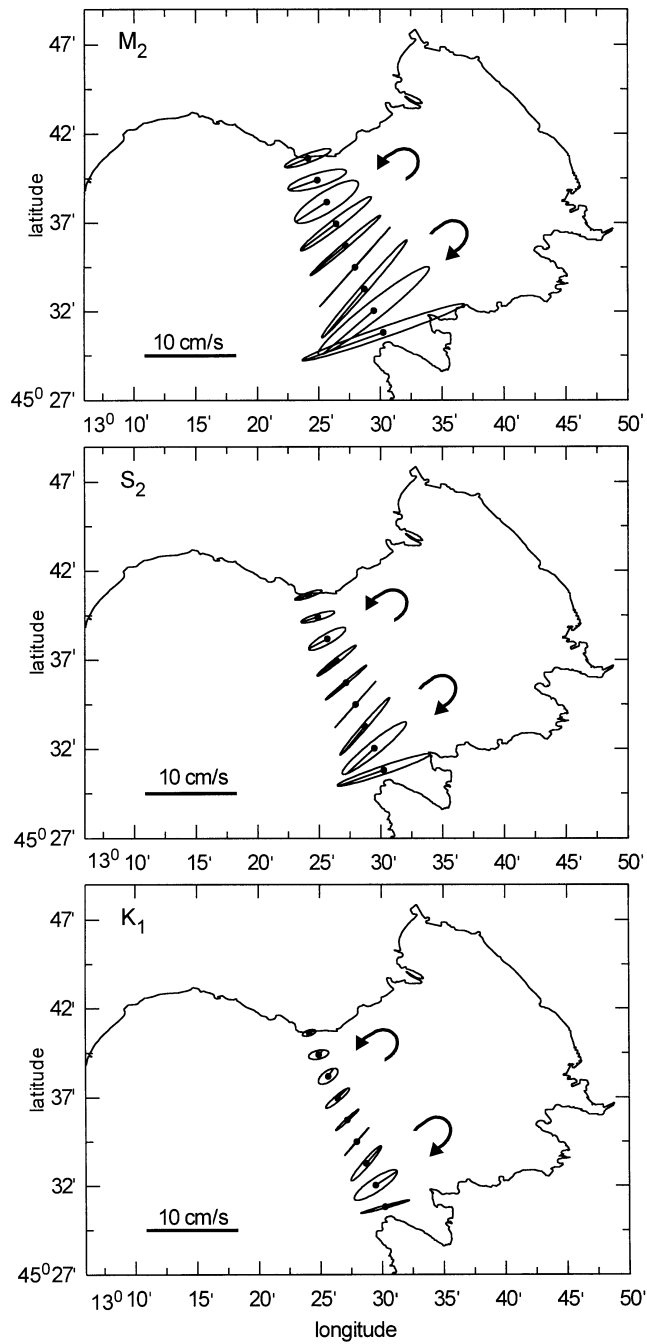
Fig. 7. – Transport velocity ellipses along the line Savudrija-Grado for the M_2 constituent (top), S_2 constituent (middle), and for the K_1 constituent (bottom). The rotation of tidal currents is marked with arrows.

distribution of the characteristics of tidal ellipses due to the smallness of the gulf. Bays of the gulf have a relatively much larger influence on the distribution of ellipse eccentricity than that found in the northern Adriatic Sea. Over most of the interior of the latter area tidal currents rotate anticlockwise and the ellipses, although still narrow, are there the broadest. Over the gulf's interior tidal ellipses are very narrow, since in that area the dynamics near the closed boundary (anticlockwise rotation) meets with the dynamics of bays (clockwise rotation).

b) Observations

Currentmeter observations for the years 1984 and 1985 enabled a comparison with the model results. Four current records at two stations (A and B) at two depths, sampled at 600 s by NBA currentmeters (table I), were taken to validate the results of the model. Both sites are in the Gulf of Trieste (fig. 3). Site A was about $3.7 \cdot 10^3$ m SW of the port of Trieste in a zone only slightly influenced by freshwater. On the contrary, site B was about $3.7 \cdot 10^3$ m southward of the outlet of the Isonzo River, in a zone of marked freshwater influence. In [24] the analysis of currentmeter data revealed the persistence and the intensity of the wind-driven currents generated by the Bora wind (ENE) during the winter period 1984-1985.

The semidiurnal and diurnal tidal bands were filtered out of the currentmeter data with an equiripple FIR (Finite Impulse Response) filter [25], with the order of 221 hours (9.2 days). The filtering, however, enlarged the data gaps. Tidal constituents were thereafter extracted out of the filtered time-series (see table I for the length of these records) with the same harmonic analysis as the one applied to the results of the run of the numerical model for the first 190 days of the year 1985.

The comparison of the model results (year 1985) with the observations is shown in table II. While the filtered records A1 and A2 are long enough for the complete separation of S_2 and K_2 constituents (182.6 days), the filtered records B1 and B2 comprise only 60 days of measurements. However, in the records A1 and A2 the wind-induced current of about 0.35 m/s, which occurred during the winter period [24], shifted the tidal frequencies due to the Doppler effect. Taking for the depth $D = 20$ m, the speed of tidal wave $c = (gD)^{1/2} \cong 14.0$ m/s, and the ratio $v/c \cong 0.025$. This ratio is the measure for the relative shift of frequencies. The relative frequency resolution of the method is $T/(\Delta TN)$, where T is the tidal period, ΔT is the period of sampling, and N is

TABLE I. – *Periods and depths of currentmeter observations at stations* A (45° 37.00′N, 13° 42.85′E; *sea-floor is at depth* $D = 21$ m) *and* B (45° 40.80′N, 13°34.00′E; $D = 14$ m) *in the Gulf of Trieste, which were considered in the analysis of model results. The length of FIR record means the number of hourly values of currentmeter data, which remained for the least-square analysis for tidal constituents after the band-pass filtration of the data with the semidiurnal and diurnal FIR filters of the order of 221 hours (see text).*

Label	Depth (m)	Start	End	Record length
A1	6	18/10/1984	12/08/1985	5016
A2	17	18/10/1984	30/08/1985	4579
B1	5	05/06/1985	13/08/1985	1441
B2	10	05/06/1985	14/08/1085	1458

TABLE II. – *Model and observed parameters from the harmonic analysis of current data at points A and B in the Gulf of Trieste. Superscripts "m" and "o" refer to model and observed values. "SAX" and "sax" refer to the semimajor and the semiminor axes of the current ellipse. The direction of maximum current speed (relative to the east axis, positive = anticlockwise) is denoted by θ_{max}, and e is the elipse eccentricity. Inside the column with observed values, upper values refer to the upper currentmeters and lower values to the lower currentmeters.*

Site	Constituent	SAX^o 10^{-2} (m/s)	SAX^m 10^{-2} (m/s)	sax^o 10^{-2} (m/s)	sax^m 10^{-2} (m/s)	e^o	e^m	θ^o_{max} (degrees)	θ^m_{max} (degrees)
A	M_2	1.26	1.62	0.06	0.02	+ 0.095	+ 0.026	43.4	27.8
		1.16		0.16		− 0.238		39.0	
A	K_2	0.22	0.25	0.02	0.03	+ 0.159	+ 0.196	40.0	28.3
		0.34		0.06		− 0.320		30.2	
A	N_2	0.43	0.27	0.07	0.01	+ 0.276	+ 0.051	27.4	27.5
		0.23		0.07		− 0.460		− 83.3	
A	S_2	0.59	0.96	0.10	0.00	+ 0.290	+ 0.006	29.9	29.2
		0.38		0.01		− 0.065		66.3	
A	K_1	0.64	0.65	0.09	0.02	+ 0.249	+ 0.060	62.8	29.6
		0.72		0.29		− 0.575		58.9	
A	P_1	0.40	0.21	0.14	0.01	+ 0.525	+ 0.090	78.0	37.1
		0.47		0.05		− 0.200		24.0	
A	O_1	0.27	0.20	0.12	0.01	+ 0.610	+ 0.060	− 58.7	34.8
		0.29		0.13		− 0.618		− 24.1	
B	M_2	2.59	3.23	0.06	0.29	+ 0.043	− 0.164	41.1	54.7
		1.98		0.50		− 0.406		68.6	
B	K_2	0.60	0.47	0.27	0.05	− 0.615	+ 0.209	− 62.3	57.7
		1.36		0.72		+ 0.694		67.1	
B	N_2	0.45	0.52	0.15	0.05	+ 0.510	+ 0.183	− 62.7	56.5
		0.70		0.21		+ 0.464		19.2	
B	S_2	0.95	1.89	0.77	0.21	− 0.898	+ 0.196	− 18.2	53.7
		2.33		1.04		+ 0.617		66.0	
B	K_1	1.02	1.06	0.43	0.12	+ 0.594	− 0.200	− 63.0	57.2
		1.23		0.30		− 0.392		39.7	
B	P_1	1.08	0.33	0.37	0.00	+ 0.512	+ 0.021	45.7	65.1
		1.41		0.38		+ 0.426		73.2	
B	O_1	0.41	0.28	0.05	0.02	+ 0.229	− 0.143	− 86.7	60.1
		0.19		0.05		− 0.389		− 26.3	

the record length. Taking $T = 24$ hours, $\Delta T = 1$ hour and $N = 5016$ (table I), the relative frequency resolution equals $2.39 \cdot 10^{-3}$ for the semidiurnal constituents. The relative Doppler shift of frequencies is therefore an order of magnitude larger than the relative frequency resolution when strong currents (of 0.35 m/s) are present. Over the whole period of observations the Doppler shift of frequencies varies in time and would

not be of this strength, but it can still shift the peaks of the tidal spectrum away from their expected positions.

The experimental amplitudes of the ellipses of tidal current and those of the model at two sites within the Gulf of Trieste are in reasonably good agreement in spite of the shortness of the experimental records with data gaps. Tidal currents, measured at sites A and B, are rather weak: only two cases out of 14 (two sites, seven constituents) have a semimajor axis of tidal current larger than 0.02 m/s (M_2 and S_2 constituents at site B). These low values of semiaxes of tidal ellipses make the comparison with the model difficult (a discussion about this will follow later). Eight values (out of 14) of the semimajor axes of current ellipses measured near the sea-floor are larger than the values of the semimajor axes (table II) measured near the sea-surface. At site A differences between observed and model semiaxes amplitudes are reasonably small with respect to the error of currentmeter observations for the constituents M_2, K_2, S_2 and K_1. The ellipse eccentricities and directions of maximum current speed are also in reasonable agreement for these major four constituents. The differences between the model values and observations are higher at site B, where the measurements took place during the season of enhanced stratification of the water column (table I), which changes the vertical structure of tides [11], and enhances the deviation of properties of tides at fixed depths from the depth averaged properties.

5. – Discussion and conclusions

Since the numerical model TRIM 2D of the tidal dynamics of the northern Adriatic Sea, with high grid resolution (556 m), was successfully calibrated for all seven major tidal constituents (an overall RMS error of all amplitudes of SSE in five ports is less than 1 cm, while for the phase shift it is less than 5°), residual features, as well as features of local dynamics in smaller regions, could be studied. In this work the mixing potential of tides over the northen Adriatic Sea has been examined, and the simulation of local dynamics has been checked against observations of the currents in the Gulf of Trieste. It has been shown with the model simulation of tides that even within a period of more than six months tides in the northern Adriatic Sea are too weak to mix the whole water column.

At this point a comment about the influence of haline stratification on the mixing capabilities of tides, related to the heat flux, seems appropriate. Over the whole model domain the amplitude of seasonal variations of temperature in the lower part of the water column is significantly lower than the amplitude near the surface [26] and that in the lower part of the water column the variable part of the vertical eddy coefficient of heat is almost negligible against the constant part, even in shallow areas of depth $D \cong$ 20 m. In plume regions, however, the coefficient of eddy diffusivity of heat is pronouncedly reduced at the halocline [16]. The surface heating/cooling effect is therefore confined to above the halocline. Moreover, in plume areas of depths $D >$ 20 m, the amount of freshwater is nearly negligible in the lower part of the water column [27, 28], especially during the summer period, when the Po river plume spreads far away from the Italian coast in the northern Adriatic Sea. All these effects contribute to the reduction of the required kinetic energy for mixing the *lower part* of the water column, which is (much) smaller than that needed for mixing the whole water column. Therefore, areas with low values of P (fig. 2), where P was obtained from the

model, are suspected to mark regions with enhanced bottom mixing. Although the stratification changes the vertical structure of tides ([11] and [29]), it is expected that regions with low values of P still indicate the existence of domains of the mixed bottom layer (near capes and promontories) at times of spring tides. The extent of these domains is, however, not clear.

The discussion about the potential of tides for mixing the lower part of the water column is also related to the vertical structure of tidal currents, which is far from being simple even for homogeneous waters. When stratification is ignored, the equations of motion for a single tidal constituent of angular frequency σ for the anticlockwise and clockwise rotating components are identical in form to the equations describing a steady flow on a rotating earth and an oscillatory flow on a nonrotating earth [11]. For a steady flow u_a above the bottom Ekman layer, the thickness of the latter depends on the "surface Rossby number" $u_a/(fz_0)$ [30], where the roughness height $z_0 = 2 \cdot 10^{-4}$ m for the muddy bottom [11]. Considering $u_a = 10$ cm/s gives $u_a/(fz_0) = 5 \cdot 10^6$. For the rotary components of a tidal constituent, the Coriolis parameter f needs to be replaced with $(f + \sigma)$ for the anticlockwise component, and with $(f - \sigma)$ for the clockwise component [11]. For the semidiurnal tide with $\sigma = 2\pi/(12 \times 3600 \text{ s})$ this gives the "modified" surface Rossby number $u_a/[(f + \sigma) z_0] = 2 \cdot 10^6$ for the anticlockwise component, and $u_a/[(f - \sigma) z_0] = 1.1 \cdot 10^7$ for the clockwise component. The corresponding thickness of the bottom Ekman is around $2 \cdot 10^4 z_0 = 4$ m for the anticlockwise motion, and around $1.1 \cdot 10^5 z_0 = 22$ m for the clockwise motion of the semidiurnal constituents. Vertical shear of the clockwise motion of tides in front of promontories and bays spreads from the bottom towards the surface, while the vertical shear of the anticlockwise motion, which is prevalent over the northern Adriatic Sea, is confined near the bottom, where the mixing occurs.

Although the parameter P has been successfully applied to continental shelf areas, it seems that it has not been used for plume areas so far, despite the studies affecting ϕ. When the main input freshwater buoyancy is from river discharge, the buoyancy is horizontally distributed by the local current system, which is also (but not only) buoyancy driven. A simple assumption about the local input of buoyancy in terms of river discharge is then not possible [31]. The tidal stirring, which decreases ϕ, competes with the tidal straining and with the estuarine circulation. Both forms of motion depend on the horizontal gradient of density and they increase ϕ. If the estuarine circulation is ignored, then tidal stirring and straining may induce short periodic bursts of mixing at the end of the flood. It was shown by model simulation [31] that the estuarine circulation enlarges the periods of stratification at neaps. These very important aspects of dynamics, which influence the mixing in plume and estuarine regions, are, however, beyond the scope of this paper.

The tidal currents in the Gulf of Trieste of the model run for the first half of 1985 were also compared with the intermittent measurements of currents that were performed at two points in the years 1984-1985. It has been shown that the agreement is satisfactory even when other agents (*e.g.* the Bora wind) affect the spectral distribution of tidal currents through the Doppler effect. At first, the model results of the run for the year 1997 were compared with the measurements of 1984-1985. The results for the year 1997 were very close to those presented in this paper (table II), and all figures (figs. 4-7) related to the dynamics in the Gulf of Trieste were practically identical to the ones presented in the paper (year 1985). For each tidal constituent at points A and B (fig. 3) the amplitudes of elevations differed for the order of 10^{-4} m and the amplitudes of transport velocity components for 10^{-3} m/s. The phases of elevations

differed for 0.2°, and the phases of velocity components for 15° (mean difference for phases of the eastern velocity components) and for 11° (for phases of the northern velocity components).

The (lunar) constituents of tides are affected by the 18.6 year nodal cycle [13]. In tidal records that span at most a year this interannual variability of tides is represented with nodal terms that are constant within the year and that modulate the amplitude and the phase of constituents on an interannual scale. In this way the numerical simulations of tides for any year can be compared with the observations from 1985. That is, for the currentmeter data the nodal factors relative to the year 1985 were considered, while for the numerical simulation of tides the nodal factors relative to the year considered in simulations have to be applied. However, slight differences that were described above may result from the weak nonlinear coupling of the constituents in advective and friction terms in the equations of motion. We may conclude that the model run for the first 190 days of the year 1985 did not show any improvement in results with respect to the results of the similar run for the year 1997, when compared with the currentmeter observations that were conducted in 1984-1885.

Another problem relates to the experimental results. When the tidal currents are weak (within the Gulf of Trieste each constituent has a semimajor axis $\leqslant 2 \cdot 10^{-2}$ m/s) the extraction of tidal signal from the currentmeter records is difficult, especially for the records of currentmeters that have been placed close to the surface, where the wind-driven currents cause the frequency shift, while waves decrease the stability of currentmeter orientation. The results of analysis when separate records of currents were joined was presented in this work (table II). However, the same type of analysis applied separately on the winter record and summer record of currents at station A shows significant differences in the orientation of major semiaxis. For most constituents they are around 20°, however, for the axis orientation of less pronounced constituents the difference may reach 133° (P_1) near the surface (6 m depth) and $\leqslant 1°$ close to the sea-floor (17 m depth). Finally, the threshold value of currentmeters (above 1 cm/s) affects the analysis in periods with calm weather and low tidal currents.

The distribution of the ellipses of tidal currents in the Gulf of Trieste was also extracted from the model. Over the larger part of the gulf, the currents rotate anticlockwise, which agrees with the analysis of tides in the semi-enclosed gulf [23]. In the southern part of the gulf's entrance, however, the Bay of Piran turns this rotation of currents into a clockwise one, in accordance with the explanation of dynamics in and in front of bays, given by [13]. The same holds also for the bays of Muggia and Panzano at the inside edges of the gulf. We may conclude that over the major part of the Gulf of Trieste tides follow the dynamics of a standing wave.

* * *

REFERENCES

[1] Defant A., *Physical Oceanography*, Vol. **2** (Pergamon Press, Oxford) 1961, p. 729.
[2] Polli S., *Atti IX Convegno Associazione Geofisica Italiana, Roma, 1959.* Also: *Publ: Inst. Talassogr.* No. 370 (1960) 1.
[3] Taylor G. I., *Proc. London Math. Soc.*, **20** (1921) 144.
[4] Hendershott M. C. and Speranza A., *Deep-Sea Res.*, **18** (1971) 959.
[5] McHugh G., *Boll. Geofis. Teor. Appl.*, **16** (1974) 322.
[6] Cavallini F., *Boll. Oceanol. Teor. Appl.*, **3** (1985) 205.
[7] Cheng R. T., Casulli V. and Gartner J. W., *Est. Coast. Shelf Sci.*, **36** (1993) 235.
[8] Malačič V., Viezzoli D. and Cushman-Roisin B., to be published in *J. Geophys. Res.*
[9] Malačič V. and Viezzoli D., in *35th Congress-Plenary Assembly of the International Commission for the Scientific Exploration of the Mediterranean sea (C.I.E.S.M.), Dubrovnik (Cavtat), Croatia*, **35** (1998) 172.
[10] Casulli V., *J. Comput. Phys.*, **86** (1990) 56.
[11] Soulsby R. L., in *The Sea*, edited by B. LeMehaute and D. M. Hanes, Vol. **B** (Wiley-Interscience, New York) 1990, pp. 523-566.
[12] Press W. H., Teukolsky S. A., Vetterling W. T. and Flannery B. P., *Numerical Recipes in FORTRAN: the Art of Scientific Computing*, 2nd Edition (Cambridge University Press, Cambridge) 1986, p. 963.
[13] Pugh D. T., *Tides, Surges and Mean Sea-Level* (John Wiley & Sons, Chishester) 1987, p. 472.
[14] Schureman P., *Manual of Harmonic Analysis and Prediction of Tides* (U.S. Government Printing Office, Washington) 1958, Reprinted 1994, p. 317.
[15] Stravisi F., *Boll. Oceanol. Teor. Appl.*, **1** (1983) 193.
[16] Bowden K. F., *The Physical Oceanography of Coastal Waters* (Ellis Horwood, New York) 1983, p. 302.
[17] Simpson J. H. and Hunter J. R., *Nature*, **250** (1974) 404.
[18] Loder J. W. and Greenberg D. A., *Cont. Shelf Res.*, **6** (1986) 397.
[19] Simpson J. H. and James I. D., in *Baroclinic Processes on Continental Shelves*, edited by C. N. K. Mooers (American Geophysical Union, Washington, DC) 1986, pp. 63-92.
[20] Brass R. L., *Hydrology* (Addison-Wesley Publ. Co., Reading) 1990, p. 643.
[21] Gonella J., *Deep-Sea Res.*, **19** (1972) 833.
[22] Mosetti R., *Boll. Oceanol. Teor. Appl.*, **4** (1986) 165.
[23] Fang Z., Ye A. and Fang G., in *Tidal Hydrodynamics*, edited by B. B. Parker (John Wiley, New York) 1991, pp. 153-168.
[24] Mosetti F. and Purga N., *Boll. Oceanol. Teor. Appl.*, 8 (1990) 251.
[25] McClellan J. H., Parks J. H. and Rabiner L. R., in *Programs for Digital Signal Processing*, edited by the Digital Signal Processing Committee IEEE Acoustic, Speech and Signal Processing Society (IEEE Press, John Wiley, New York) 1979, pp. 5.1 1-5.1 13.
[26] Malačič V., *Oceanol. Acta*, **14** (1991) 23.
[27] Mosetti F. and Lavenia A., *Boll. Geof. Teor. Appl.*, **11** (1969) 191.
[28] Orlić M., Gačić M. and La Violette P. E., *Oceanol. Acta*, **15** (1992) 109.
[29] Prandle D., in *Tidal Hydrodynamics*, edited by B. B. Parker (John Wiley, New York) 1991, pp. 125-152.
[30] Cushman-Roisin B. and Malačič V., *J. Phys. Oceanogr.*, **27** (1997), 1967.
[31] Simpson J. H., Brown J., Matthews J. and Allen G., *Estuaries*, **13** (1990) 125.